PROCEEDINGS OF SPIE

SPIEDigitalLibrary.org/conference-proceedings-of-spie

Fabrication of 3-D light concentrating microphotonic structures by anisotropic wet etching of silicon

Bidney, Grant, Jin, Boya, Deguzman, Lou, Hutchens, Thomas, Duran, Joshua, et al.

Grant W. Bidney, Boya Jin, Lou Deguzman, Thomas C. Hutchens, Joshua M. Duran, Gamini Ariyawansa, Igor Anisimov, Nicholaos I. Limberopoulos, Augustine M. Urbas, Kenneth W. Allen, Sarath D. Gunapala, Vasily N. Astratov, "Fabrication of 3-D light concentrating microphotonic structures by anisotropic wet etching of silicon," Proc. SPIE 12012, Advanced Fabrication Technologies for Micro/Nano Optics and Photonics XV, 120120B (5 March 2022); doi: 10.1117/12.2610426

SPIE.

Event: SPIE OPTO, 2022, San Francisco, California, United States

Fabrication of 3-D Light Concentrating Microphotonic Structures by Anisotropic Wet Etching of Silicon

Grant W. Bidney,[1,2] Boya Jin,[1] Lou Deguzman,[1] Thomas C. Hutchens,[1] Joshua M. Duran,[2] Gamini Ariyawansa,[2] Igor Anisimov,[2] Nicholaos I. Limberopoulos,[2] Augustine M. Urbas,[3] Kenneth W. Allen,[4] Sarath D. Gunapala,[5] and Vasily N. Astratov[1,2,*]

[1]*Department of Physics and Optical Science, Center for Optoelectronics and Optical Communications, University of North Carolina at Charlotte, Charlotte, NC 28223-0001, USA*

[2]*Air Force Research Laboratory, Sensors Directorate, Wright Patterson AFB, OH 45433, USA*

[3]*Air Force Research Laboratory, Materials and Manufacturing Directorate, Wright-Patterson AFB, OH 45433, USA*

[4]*Advanced Concepts Laboratory, Georgia Tech Research Institute, Georgia Institute of Technology, Atlanta, GA 30332, USA*

[5]*Jet Propulsion Laboratory, California Institute of Technology, 4800 Oak Grove Dr., Pasadena, California 91030, USA*

**Tel: 1 (704) 687 8131, Fax: 1 (704) 687 8197, E-mail: astratov@uncc.edu*

ABSTRACT

Silicon has been commonly used in the microelectromechanical systems (MEMS) community for the past sixty years, and anisotropic wet etching with tetramethylammonium hydroxide (TMAH) has been central to these fabrication efforts. It has been shown anisotropic wet etching of silicon is an ideal method to rapidly fabricate components with huge production volume, and low cost. Although TMAH has been commonly used to create integrated circuits, the technology hasn't been fully explored for optical applications. Four types of light concentrating arrays were fabricated with this technology in this work: (i) micropyramids with 54.7˚ sidewall angle, (ii) microcones with 45˚ sidewall angle, (iii) inverted square pyramids with 54.7˚ sidewall angle, and (iv) inverted triangular pyramids with different sidewall angles. The 54.7˚ sidewall angle arrays have smooth sidewalls due to etching with TMAH, which reduces scattering loss. The 3-D microphotonic structures were created through a comparable fabrication protocol, but require different photoresists, mask alignments, and if the surfactant Triton X-100 was utilized during the etch. The fabricated structures can be either heterogeneously integrated with front-illuminated focal plane arrays (FPAs) created in material systems with high quantum efficiency, or be monolithically integrated with metal/silicide Schottky barrier photodetectors for operation in short-wave infrared (SWIR) or mid-wave infrared (MWIR) regimes. The light concentrating capability of the proposed structures was tested by finite-difference time-domain modeling. Experimentally, the formation of photonic nanojets at the tips of micropyramids was demonstrated using illumination by a 2.96 μm wavelength Er:YAG laser.

Keywords: silicon photonics, infrared imaging, light concentrators, microphotonics, focal plane arrays, dielectric resonance, MEMS

1. INTRODUCTION

Within the past decade, two ideas appeared to improve different photodetectors by implementing light concentrating structures with three-dimensional geometry based on normal [1] or inverted [2] Si micropyramidal arrays with metal coating the sidewall surface. These designs concentrate light towards the nanometer scale apex, and are based on converting incident photons into plasmons or localized surface plasmon resonance (LSPR) excitations, where the plasmons are adiabatically compressed towards the tips leading to the generation of electron-hole pairs. The Si light concentrators couple electromagnetic energy into the compact photodetectors to intensify the signal and improve the signal-to-noise ratio (SNR) of infrared focal plane arrays (FPAs). In the case of normal micropyramidal light concentrators, a photoresponse increase of nearly a hundred times compared to the conventional flat geometry was reported [1]. In the case of inverted micropyramidal light concentrators, a photoresponse increase of approximately forty times compared to a flat photodetector was reported [2]. Concurrently, light concentrators via dielectric components like microspheres [3-6] or microcones [7-12] in contact with FPAs were proposed and realized. Analogous to the

Advanced Fabrication Technologies for Micro/Nano Optics and Photonics XV, edited by Georg von Freymann, Eva Blasco, Debashis Chanda, Proc. of SPIE Vol. 12012, 120120B · © 2022 SPIE · 0277-786X · doi: 10.1117/12.2610426

aforementioned plasmonic light concentrators, anisotropic wet etching with Si was realized to fabricate high-index microcones [9-11]. In addition to increasing the light collected, these structures resonantly trap photons inside the microcones resulting in notable spectral resonance peaks with the integrated photodetectors. These light concentrators can be used to improve the SNR by reducing the photodetector size, therefore reducing the thermal noise proportional to the detector size, and increasing the collection efficiency in uncooled mid-wave infrared (MWIR) or short-wave infrared (SWIR) detectors [13, 14].

Many of these light-concentrating microphotonic structures are fabricated by Si anisotropic wet etching originally developed by the microelectromechanical systems (MEMS) community. This was done by using different photoresists, etchants such as potassium hydroxide (KOH) or tetramethylammonium hydroxide (TMAH) for different geometries depending on the crystallographic orientation of the wafer, and additives to the etchant like isopropyl alcohol (IPA) or Triton X-100 to improve surface quality or reduce undercutting of the silica layer [15-20]. The optical applications that have been studied include resonator cavities, micro mirrors, beam splitters, and diffraction gratings [21]. However, these structures have not been fully explored as light concentrators, back reflectors [22, 23], or other photonic microstructures. It has been shown that Si anisotropic wet etching is an ideal method to rapidly fabricate components with huge production volume, and low cost.

In this work, four types of light concentrating arrays were fabricated with this technology: (i) micropyramids with 54.7˚ sidewall angle, (ii) microcones with 45˚ sidewall angle, (iii) inverted square pyramids with 54.7˚ sidewall angle, and (iv) inverted triangular pyramids with different sidewall angles. The light concentrating capability of type (i) was tested by finite-difference time-domain (FDTD) modeling. The optical characterization demonstrated the formation of photonic nanojets at the tips of micropyramids by illumination with a 2.96 μm wavelength Er:YAG laser. The fabricated structures can be either heterogeneously integrated with high quantum efficiency front-illuminated FPAs or be monolithically integrated with metal/silicide Schottky barrier photodetectors to function in the SWIR or MWIR regimes [24-26].

2. FABRICATION

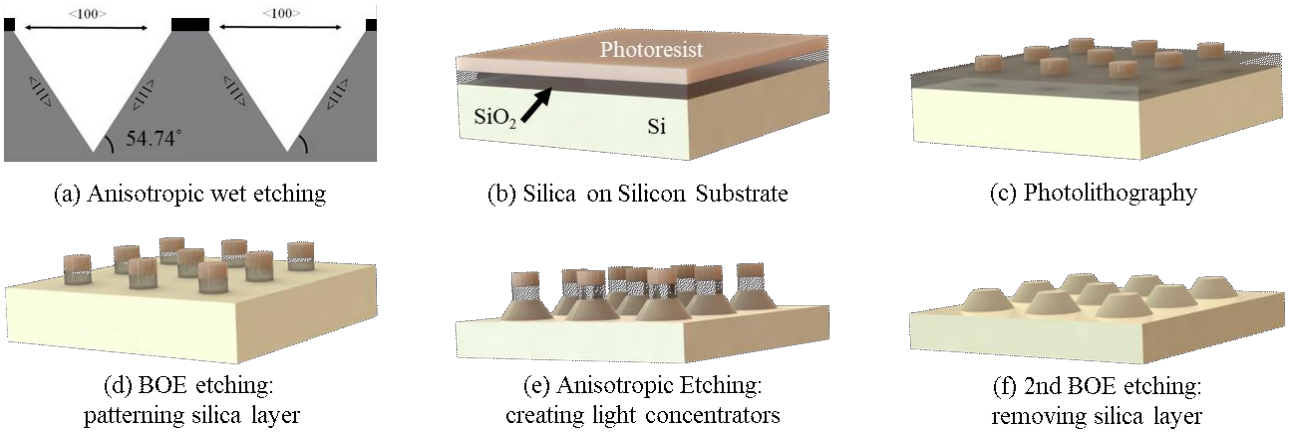

Figure 1. (a) Side view of a (100) Si wafer with thermal SiO_2 caps where the (111) crystalline planes were wet etched to form Si micropyramids with 54.74˚ sidewall angle. (b-f) Diagrams depicting the fabrication steps to create Si light concentrating arrays by anisotropic wet etching with TMAH.

The 3-D light concentrating microphotonic structures were created through a comparable fabrication protocol, but require different photoresists, mask alignments, and if the surfactant Triton X-100 was utilized which reduces the rate TMAH undercuts the SiO_2 layer during the anisotropic wet etch step. Fig. 1 depicts the typical fabrication protocol. The initial substrate was a double-side polished (DSP) (100) Si wafer with thermal SiO_2 on both sides. To prepare the wafer for photolithography as shown in Fig. 1(b), the surface was cleaned with IPA and a dehydration bake was performed on a hot plate at 115˚ C for 75 seconds. Hexamethyldisilizane (HMDS) was spin coated at 4000 RPM for 45 seconds when positive photoresists were used, as an adhesion promoter to ensure a quality transfer of the pattern. Negative photoresists adhere well enough where an adhesion promoter is not required. Microposit S1813 positive photoresist was spin coated, exposed, and developed with CD-26 to create the patterns shown in Fig. 2(a, b, d). NR9-1500 negative photoresist was spin coated, exposed, and developed with RD6 to create the pattern shown in Fig. 2(c). These steps follow the diagram shown in Fig. 1(c). After the photolithography was completed, the wafer underwent a 4

minute O_2 plasma ash to remove any residual photoresist that may not have been removed during developing. The photoresist pattern was then transferred to the SiO_2 layer with a 10:1 buffered oxide etch (BOE) as shown in Fig. 1(d). The samples were then immediately submerged in an 80˚ C solution consisting of TMAH with 0.2% v/v Triton X-100 surfactant for the arrays shown in Fig. 2(e, h), or submerged in TMAH alone for the arrays shown in Fig. 2(f, g), as depicted in Fig. 1(e). Lastly, the samples were placed in a second BOE bath to remove the SiO_2 pattern as shown in Fig. 1(f), resulting in the four 3-D light concentrating microphotonic structures shown in the scanning electron microscope (SEM) images in the four columns of Fig. 2. The first column are images corresponding to 2.4 µm top and 15.0 µm pitch Si micropyramids with 54.7˚ sidewall angles. The second column are images corresponding to 7.3 µm top and 30.0 µm pitch Si microcones with ~45˚ sidewall angles. The third column are images corresponding to inverted Si square micropyramids with 54.7˚ sidewall angles. The microphotonic structures with 54.7˚ sidewall angles had masks aligned to the <110> direction on the (100) Si wafer for etching along the (111) crystalline planes. The fourth column are images corresponding to 23.3 µm long and 20.7 µm wide Si triangular micropyramids with different sidewall angles. These microphotonic structures had one side of the mask aligned to the <110> direction, resulting in a 54.7˚ sidewall angle, and two sides of the mask not aligned to the <110> direction, resulting in ~48˚ sidewall angles.

Therefore, the performed fabrication demonstrated the numerous advantages of Si anisotropic wet etching for fabricating 3-D light concentrating microphotonic structures with applications in Si photonics: a) simultaneous rapid production of large-scale 3-D normal or inverted micropyramidal arrays, b) control over the light concentrator sidewall angle depending on the mask orientation for arrays fabricated on a (100) wafer, and c) smooth sidewall surface for the 54.7˚ angles to reduce scattering losses for optical applications. It has been shown Si anisotropic wet etching is an ideal method to rapidly fabricate components with massive-scale production volume, and low cost.

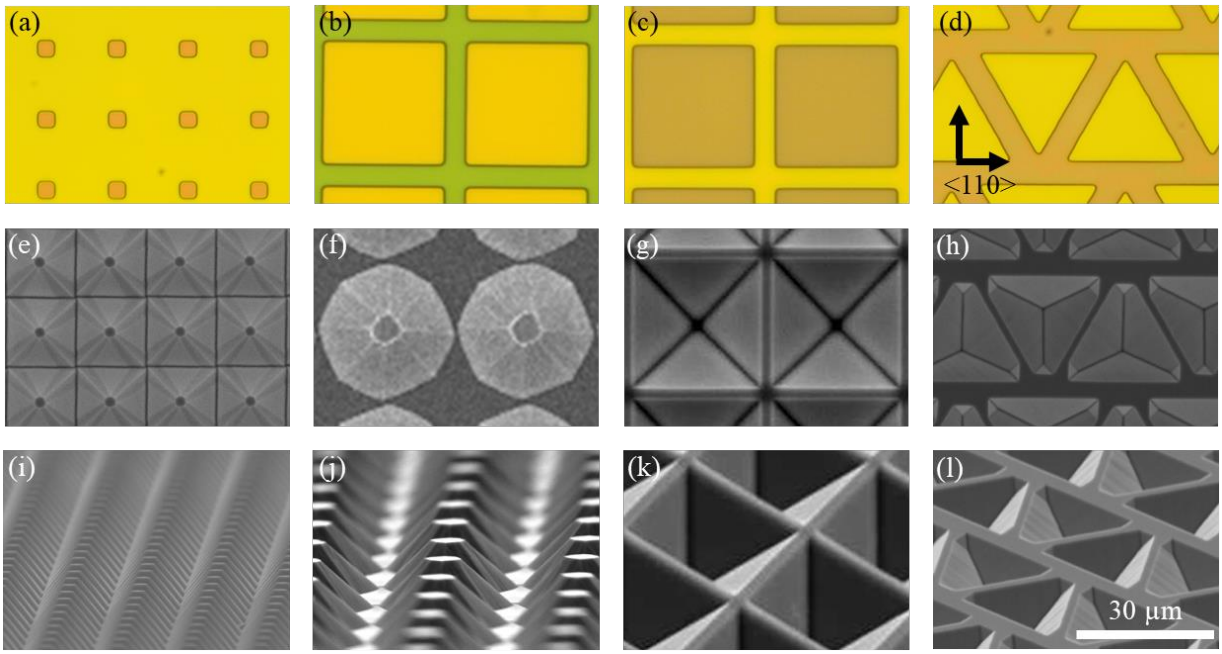

Figure 2. The first column represents (a) photoresist pattern and SEM images of the fabricated normal micropyramids with 54.7˚ sidewall angle (2.4 µm top and 15.0 µm pitch) at (e) normal and (i) oblique incidence. The second column represents similar images (b, f. j), respectively, in the case of fabrication of normal microcones with 45˚ sidewall angle (7.3 µm top and 30.0 µm pitch). The third column represents similar images (c, j, k), respectively, in the case of fabrication of inverted square pyramids with 54.7˚ slope of the sidewall surface. The fourth column represents similar images (d, h, l), respectively, in the case of fabrication inverted triangular (23.3 µm longer and 20.7 µm shorter sides) pyramids with different sidewall angles. One side of the triangular mask was aligned to the <110> direction, resulting in a 54.7˚ slope of the corresponding sidewall. The other two sides of the mask were not aligned to the <110> direction, resulting in ~48˚ slopes of the corresponding sidewalls.

3. OPTICAL CHARACTERIZATION

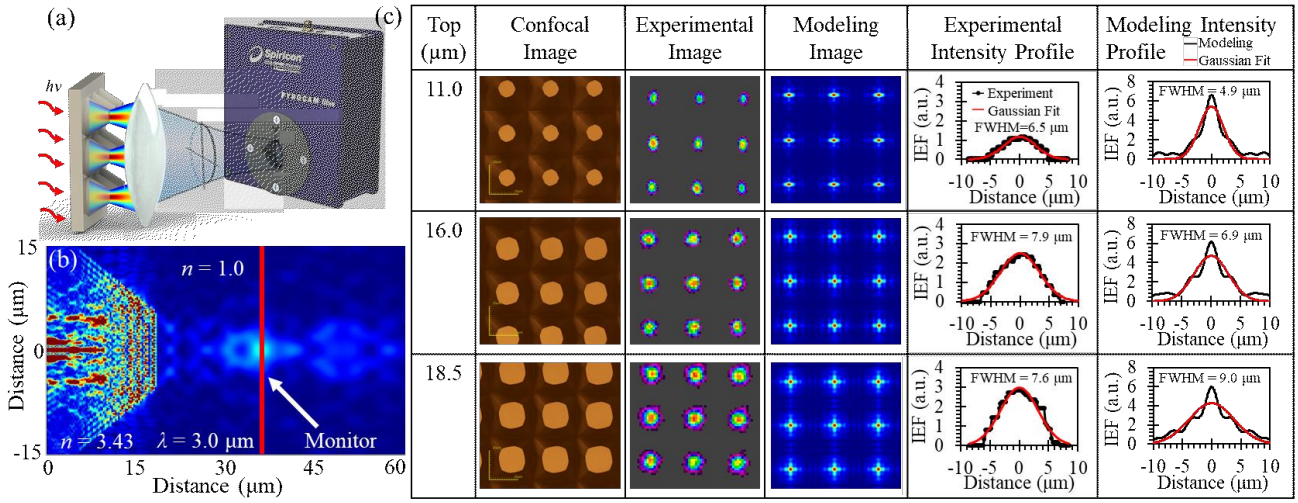

Figure 3. (a) Schematic of the setup with illumination provided by a 2.96 μm wavelength Sheaumann Er:YAG laser and imaging provided by the Spiricon camera. (b) Electromagnetic field map calculated for 11.0 μm top, 30.0 μm pitch Si micropyramid concentrating light into air. The wavelength is 3.0 μm, and the monitor position changes with pyramid geometry. (c) Table containing the following six columns (from left to right): sizes of the top base of micropyramids, 3-D confocal microscope images of the arrays, Spiricon camera images, modeling images, experimental intensity profiles, and modeling intensity profiles for three micropyramids with 30.0 μm pitch. The intensity enhancement factor (IEF) is defined as IEF = $I_{pyramid}$ /I_{ref}, where $I_{pyramid}$ is the intensity with light concentrator, I_{ref} is the reference intensity without concentrator.

In order to demonstrate the light concentrating ability, experimental optical characterization was performed for the Si micropyramidal light concentrators. The light source was a 2.96 μm wavelength Sheaumann Er:YAG laser with a ~2 mm aperture collimated beam which was focused onto the polished backside surface of the micropyramidal arrays through a 12.7 mm diameter with 12.7 mm focal length CaF_2 lens. The light propagated through the sample, concentrated near the top of the micropyramids, collected by the 25 mm diameter with 12.5 mm focal length 3 – 5 μm antireflective coated Ge aspheric lens, and focused onto the Spiricon camera as shown in Fig. 3(a). The goal of this optical characterization was to experimentally observe the concentrated spatial patterns of the light produced by the micropyramids. Since Si is primarily transmissive in the MWIR range, the light propagates without significant absorption. The light trapping inside the micropyramids can be complicated due to the resonant properties previously predicted [9], and are outside the scope of this research due to the single wavelength source.

Visualization of the concentrated light for micropyramids with 11.0, 16.0, and 18.5 μm top with 30.0 μm pitch is illustrated in Fig. 3(c). The experimental MWIR images were obtained at the narrowest waists of the focused beams near the tops of the micropyramids. The experimental intensity profiles were fitted using the Gaussian distribution function to determine the associated full width at half maximum (FWHM). The diffraction-limited FWHM for this system is approximately ~ λ/(2NA) = 2.1 μm, where NA = 1/√2 is a numerical aperture of the lens. To analyze the light concentrating capability, a factor called the intensity enhancement factor (IEF) was introduced based on the following definition: IEF = $I_{pyramid}$ /I_{ref}, where $I_{pyramid}$ is the intensity with light concentrator, I_{ref} is the average intensity without concentrator. The 18.5 μm top micropyramid was found to have a peak IEF = 3.0 with FWHM = 7.6 μm. The 16.0 μm top micropyramid was found to have a peak IEF = 2.5 with FWHM = 7.9 μm. Finally, the 11.0 μm top micropyramid was found to have a peak IEF = 1.2 with FWHM = 6.5 μm.

The corresponding Ansys/Lumerical FDTD modeling depicts the observed beam-concentration properties of the micropyramids, but it predicts even larger IEF factors with tighter beam waists as the micropyramid top size decreases (Fig. 3). The electromagnetic field map shown in Fig. 3(b) corresponds to an 11.0 μm top with 30.0 μm pitch pyramid. It was calculated with periodic boundary conditions to consider the periodicity of the arrays. The normal incidence simulation wavelength is 3.0 μm, and the square power monitor position is located at the position of highest intensity. Therefore, the monitor position has an adjustable position spanning the entire width of the 30.0 μm simulation region. The micropyramids with 18.5, 16.0, and 11.0 μm tops have calculated IEFs with the progressively higher and narrower peaks. For 18.5 μm tops the IEF peak has magnitude 6.0 with the Gaussian FWHM = 9.0 μm. For 16.0 μm top

micropyramid the IEF peak increases to 6.2 with Gaussian FWHM = 6.9 μm. Finally, for 11.0 μm top micropyramid the IEF peak reaches 6.6 with Gaussian FWHM = 4.9 μm.

Thus, the experimental values of FWHMs at the narrowest waist of the focal beams were found to be in a reasonable agreement with the corresponding theoretical calculations. The fact that on average the experiment tends to provide slightly wider FWHMs (except for the case of 18.5 μm pyramids) can be related to a finite diffraction-limited resolution ~ λ/(2NA) = 2.1 μm of our imaging system. It can be also related to finite sizes of the pixels of our imaging camera. More serious disagreement was observed for the IEF peaks which are expected to slightly increase with the reduced size of the top base of micropyramids according to calculations, but an opposite trend was observed experimentally. This behavior can be explained by the optical losses due to light scattering on the roughness of the sidewall surface of micropyramids which can play progressively more significant role for pyramids with smaller tops and which was not considered in our calculations.

We illustrated the optical properties of structures fabricated by anisotropic wet etching of Si for only the first type of micropyramidal arrays with 54.7˚ sidewall angle and showed their strong light concentrating capability. This is quite a remarkable property which can be used for enhancing collection of photons with large angle-of-view on pixels of MWIR FPAs [7-9]. In turn, it allows for the reduction of pixel size (and, consequently, their thermal noise) without sacrificing the sensitivity of the sensor array. Similar applications can be proposed for other types of the arrays fabricated in this work. It should be noted, however, that the inverted arrays would require a deposition of a thin layer of metals on the inner surface of micropyramidal dents which would enable excitation of localized surface plasmon resonances (LSPR) which can be used for enhancing the photoresponsivity [2]. The purpose of this work was to show the high potential of anisotropic wet etching of Si for producing such structures at low cost in a way amenable for large scale monolithic integration with silicon photonics or heterogeneous integration with quantum detectors with very high quantum yield fabricated in different material systems.

4. CONCLUSIONS

Our experimental optical characterization results show that anisotropic wet etching of Si produces high quality light concentrating micropyramidal arrays for optical applications. The performed fabrication demonstrated the advantages of Si anisotropic wet etching though the rapid fabrication of four 3-D light concentrating microphotonic structures with different sidewall angles, and smoothness to reduce scattering losses for optical applications. The light concentrating capability of Si micropyramidal arrays with 54.7˚ sidewall angle was tested by FDTD modeling, and experimental optical characterization demonstrates the formation of photonic nanojets at the tips of micropyramids by illumination with a 2.96 μm wavelength Er:YAG laser. The efficiency and concentration ability of these light concentrators require more research for exhaustive conclusions.

ACKNOWLEDGMENT

This work was supported by Center for Metamaterials, an NSF I/U CRC, award number 1068050. Part of this work was carried out at the Jet Propulsion Laboratory, California Institute of Technology, under a contract with the National Aeronautics and Space Administration (80NM0018D0004).

REFERENCES

[1] B. Desiatov, I. Goykhman, N. Mazurski, J. Shappir, J. Khurgin, and U. Levy, "Plasmonic enhanced silicon pyramids for internal photoemission Schottky detectors in the near-infrared regime," Optica 2, 335-338 (2015).

[2] H.-J. Syu, H.-C. Chuang, M.-J. Lin, C.-C. Cheng, P.-J. Huang, and C.-F. Lin, "Ultra-broadband photoresponse of localized surface plasmon resonance from Si-based pyramid structures," Photonics Res. **7**(10), 1119–1126 (2019).

[3] V. N. Astratov, K. W. Allen Jr., N. I. Limberopoulos, A. Urbas, and J. M. Duran, "Photodetector focal plane array systems and methods," patent application14/587,068 filed on 12/31/2014. U.S. patent 9,362,324 (7 June 2016).

[4] K. W. Allen, F. Abolmaali, J. M. Duran, G. Ariyawansa, N. I. Limberopoulos, A. M. Urbas, and V. N. Astratov, "Increasing sensitivity and angle-of-view of mid-wave infrared detectors by integration with dielectric microspheres," Appl. Phys. Lett. **108**(24), 241108 (2016).

[5] F. Abolmaali, A. Brettin, A. Green, N. I. Limberopoulos, A. M. Urbas, and V. N. Astratov, "Photonic jets for highly efficient mid-IR focal plane arrays with large angle-of-view," Opt. Express **25**(25), 31174–31185 (2017).
[6] A. Brettin, F. Abolmaali, N. I. Limberopoulos, A. Green, I. Anisimov, A. M. Urbas, et al., "Towards fabrication of mid-IR FPAs with enhanced sensitivity and reduced dark current by using integration with microspherical arrays," *NAECON 2018 - IEEE National Aerospace and Electronics Conference*, 2018, pp. 533-535, doi: 10.1109/NAECON.2018.8556727.
[7] V. N. Astratov, A. Brettin, N. I. Limberopoulos, and A. Urbas, "Photodetector Focal Plane Array systems and methods based on microcomponents with arbitrary shapes," 06/13/2017. U.S. patent 10,585,238 (March 10, 2020).
[8] A. Brettin, N. I. Limberopoulos, I. Anisimov, A. M. Urbas and V. N. Astratov, "Microconical arrays as novel light-concentrating structures for enhancing sensitivity, angle-of-view, and reducing dark current of mid-IR FPAs," *NAECON 2018 - IEEE National Aerospace and Electronics Conference*, 2018, pp. 496-498, doi: 10.1109/NAECON.2018.8556800.
[9] B. Jin, G. Bidney, A. Brettin, N. Limberopoulos, J. Duran, G. Ariyawansa, I. Anisimov, A. Urbas, S. Gunapala, H. Li, and V. Astratov, "Microconical silicon mid-IR concentrators: spectral, angular and polarization response," Opt. Express 28, 27615-27627 (2020).
[10] B. Jin, G. W. Bidney, N. I. Limberopoulos, J. M. Duran, G. Ariyawansa, I. Anisimov, et al., "Design of Si Micro-Cone Light Concentrators for Heterogeneous Integration with MWIR FPAs," *2020 22nd International Conference on Transparent Optical Networks (ICTON)*, 2020, pp. 1-4, doi: 10.1109/ICTON51198.2020.9203159.
[11] B. Jin, G. W. Bidney, A. Brettin, N. I. Limberopoulos, I. Anisimov, A. M. Urbas, "High-index micro-cones for focusing and concentrating light in MWIR focal plane arrays," *2019 IEEE National Aerospace and Electronics Conference (NAECON)*, 2019, pp. 665-668, doi: 10.1109/NAECON46414.2019.9057919.
[12] B. Jin, A. Brettin, G. W. Bidney, N. I. Limberopoulos, J. M. Duran, G. Ariyawansa, I. Anisimov, A. M. Urbas, K. W. Allen, S. D. Gunapala, and V. N. Astratov, "Light-harvesting microconical arrays for enhancing infrared imaging devices: Proposal and demonstration," Appl. Phys. Lett. **119**, 051104 (2021).
[13] A. Rogalski, "Progress in focal plane array technologies," Prog. Quantum Electron. **36**(2-3), 342–473 (2012).
[14] S. Zhang, A. Soibel, S. A. Keo, D. Wilson, S. B. Rafol, D. Z. Ting, A. She, S. D. Gunapala, and F. Capasso, "Solid-immersion metalenses for infrared focal plane arrays," Appl. Phys. Lett. **113**(11), 111104 (2018).
[15] I. Zubel and I. Barycka, "Silicon anisotropic etching in alkaline solutions I. The geometric description of figures developed under etching Si (100) in various solutions," Sens. Actuators, A **70**(3), 250–259 (1998).
[16] H. Lu, H. Zhang, M. Jin, T. He, G. Zhou, and L. Shui, "Two-Layer Microstructures Fabricated by One-Step AnisotropicWet Etching of Si in KOH Solution," Micromachines **7**(2), 19 (2016).
[17] P. Pal and K. Sato, "A comprehensive review on convex and concave corners in silicon bulk micromachining based on anisotropic wet chemical etching," Micro and Nano Syst. Lett. **3**(1), 6 (2015).
[18] O. Tabata, R. Asahi, H. Funabahi, K. Shimaoka, and S. Sugiyama, "Anasotropic etching of silicon in TMAH solutions," Sens. Actuators, A **34**(1), 51–57 (1992).
[19] Y. Fan, P. Han, P. Liang, Y. Xing, Z. Ye, and S. Hu, "Differences in etching characteristics of TMAH and KOH on preparing inverted pyramids for silicon solar cells," Appl. Surf. Sci. **264**, 761–766 (2013).
[20] X. Chen, R. S. Patel, J. A. Weibel, and S. V. Garimella, "Coalescence-induced jumping of multiple condensate droplets on hierarchical superhydrophobic surfaces," Sci. Rep. **6**(1), 18649 (2016).
[21] F. Joachim, "Shape and functional elements of the bulk silicon microtechnique: A manual of wet-etched silicon structures," Berlin: Springer, 2005.
[22] T. Sherlock, A. Nasrullah, J. Litvinov, E. Cacao, J. Knoop, S. Kemper et al., "Suspended, micron-scale corner cube retroreflectors as ultra-bright optical labels," J. Vac. Sci. Technol. B Nanotechnol Microelectron. 29 (2011), doi:10.1116/1.3656801.
[23] B. C. Park, T. B. Eom, and M. S. Chung, "Polarization properties of cube-cornerretroreflectors and their effects on signal strengthand nonlinearity in heterodyne interferometers," Appl. Optics **35**(22), 4372-4380 (1996).
[24] J. Duran and A. Sarangan, "Schottky- barrier photodiode internal quantum efficiency dependence on nickel silicide film thickness," IEEE Photonics J. **11**(1), 1–15 (2019).
[25] J. Duran, "Silicon-based infrared photodetectors for low-cost imaging applications," Ph.D. thesis (University of Dayton, 2019). Available at: https://etd.ohiolink.edu/pg_10?::NO:10:P10_ETD_SUBID:179778
[26] C. L. Tan and H. Mohseni, "Emerging technologies for high performance infrared detectors," Nanophotonics **7**(1), 169–197 (2018).